

Low-temperature interface engineering for high-quality ZnO epitaxy on Si(111) substrate

X. N. Wang, Y. Wang, Z. X. Mei, J. Dong, Z. Q. Zeng, H. T. Yuan, T. C. Zhang, and X. L. Du^{a)}

Beijing National Laboratory for Condensed Matter Physics, Institute of Physics, Chinese Academy of Sciences, Beijing 100080, China

J. F. Jia and Q. K. Xue^{b)}

Institute of Physics, Chinese Academy of Sciences, Beijing 100080, China and Department of Physics, Tsinghua University, Beijing 100084, China

X. N. Zhang and Z. Zhang

Beijing University of Technology, Beijing 100022, China

Z. F. Li and W. Lu

National Laboratory for Infrared Physics, Shanghai Institute of Technical Physics, Chinese Academy of Sciences, Shanghai 200083, China

(Received 30 November 2006; accepted 11 March 2007; published online 11 April 2007)

ZnO(0001)/Si(111) interface is engineered by using a three-step technique, involving low-temperature Mg deposition, oxidation, and MgO homoepitaxy. The double heterostructure of MgO(111)/Mg(0001)/Si(111) formed at $-10\text{ }^{\circ}\text{C}$ prevents the Si surface from oxidation and serves as an excellent template for single-domain ZnO epitaxy, which is confirmed with *in situ* reflection high-energy electron diffraction observation and *ex situ* characterization by transmission electron microscopy, x-ray diffraction, and photoluminescence. The low-temperature interface engineering method can also be applied to control other reactive metal/Si interfaces and obtain high-quality oxide templates accordingly. © 2007 American Institute of Physics. [DOI: 10.1063/1.2722225]

Recently, ZnO has been considered as one of the most promising candidates for the materials used in short-wavelength optoelectronic devices because of its wide band gap of 3.37 eV and high exciton binding energy of 60 meV at room temperature.¹ Much attention has been paid on development of growth techniques to obtain high-quality single-crystalline ZnO films.^{2,3} In those studies, sapphire is extensively used as substrate, analogous with the case of GaN epitaxy on sapphire. For potential integration of ZnO-based optoelectronic devices with the well-developed Si technologies, the epitaxial growth of ZnO films on Si substrate is also highly desirable. Si substrate has advantage over sapphire for ZnO epitaxy thanks to its lower cost, larger size, better crystal quality, and smaller lattice mismatch (-15.4% vs 18.3%). However, the easy oxidation of silicon surface, the formation of silicides even at room temperature (RT),⁴ and the big lattice mismatch between ZnO and Si severely influence the quality of ZnO films. An appropriate interface engineering such as prevention of the Si surface from oxidation and/or deposition of some buffer layer before ZnO growth is necessary for achieving high-quality ZnO epitaxy. A MgO buffer layer grown at $350\text{ }^{\circ}\text{C}$ has been used to prepare ZnO films on Si, but the film quality needs to be improved because of the formation of magnesium silicide.⁵ Though some groups attempted to use nonoxides as buffer layers, such as ZnS,⁶ SiC,⁷ and Si₃N₄,⁸ the preparation of high-quality ZnO films on Si remains a formidable challenge.

In this work, we have systematically investigated the behavior of Mg on Si(111)- 7×7 surface deposited at different temperatures from -30 to $400\text{ }^{\circ}\text{C}$ by *in situ* reflection high-energy electron diffraction (RHEED) and *ex situ* cross-sectional high resolution transmission electron microscopy (HRTEM). The results show that the interdiffusion between Mg and Si could be suppressed completely at low temperature (LT). As a result, a sharp interface of Mg(0001)/Si(111) is obtained. Based on this finding, a LT interface engineering technique is developed to prepare an excellent MgO template for the growth of high-quality ZnO films.

Our ZnO films were grown on 2 in. Si(111) wafer by using a rf-plasma assisted molecular beam epitaxy (MBE) system (OmniVac).^{2,3} Element Zn (6N) and Mg (5N) beams were supplied with two commercial Knudsen cells (CreaTech), respectively. Active oxygen radicals (O^{*}) were produced by a rf-plasma system (SVTA) using high-purity oxygen gas (5N5), which was further purified with an oxygen gas purifier (Saes) before its entry to the UHV chamber. Before loaded into the growth chamber, the Si wafers were degreased in acetone and trichloroethylene, then etched by 5% HF solution for 5 min, and rinsed in de-ionized water. Mg was deposited on Si(111) with a rate of 0.2 \AA/s under ultrahigh vacuum condition and the substrate temperature was held at 400, 200, 100, 40, 0, -10 , -20 , and $-30\text{ }^{\circ}\text{C}$, respectively, which was obtained by controlling the power supply of the substrate heater and/or liquid-nitrogen flow in cryoshield. The MgO growth rate was 0.2 \AA/s , and ZnO epilayers were grown at $650\text{ }^{\circ}\text{C}$ with a rate of 0.8 \AA/s . The flow rate of oxygen gas during oxidation and growth of MgO and ZnO films were maintained at 2.0 SCCM (SCCM denotes cubic centimeter per minute at STP).

^{a)}Electronic mail: xldu@aphy.iphy.ac.cn

^{b)}Electronic mail: qkxue@aphy.iphy.ac.cn

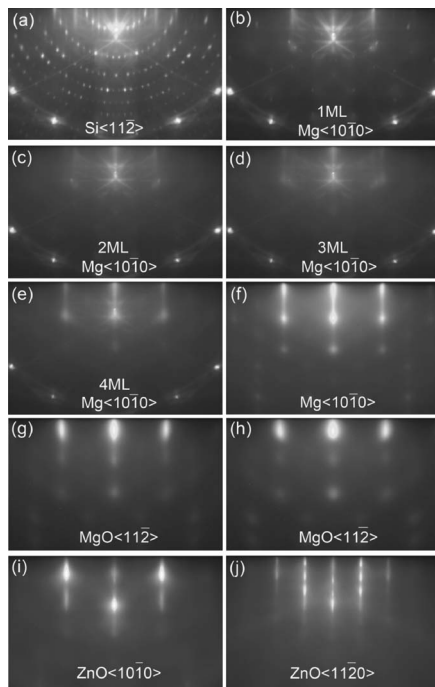


FIG. 1. RHEED patterns with incident electron beams along $\langle 11\bar{2} \rangle_{\text{Si}}$ azimuths, obtained from Si(111)- 7×7 surface (a); after Mg growth at -10°C with Mg coverages of 1 ML (b), 2 ML (c), 3 ML (d), 4 ML (e), and 4 nm (f); after exposure of Mg layer to O^* at -10°C for 20 min (g); after homoepitaxial growth of MgO at -10°C (h); and after ZnO epitaxial growth at 650°C for 3.5 h along $\langle 11\bar{2} \rangle_{\text{Si}}$ and $\langle 10\bar{T} \rangle_{\text{Si}}$ electron-beam azimuths [(i) and (j)], respectively.

The Si(111) substrate was pretreated in the UHV growth chamber to obtain the 7×7 reconstructed surface by using the well-established annealing method.⁵ The well-defined Si(111)-(7×7) reconstruction shown in Fig. 1(a) indicates a clean surface before Mg deposition. In order to understand the temperature-dependent behavior of Mg on the Si(111)-(7×7) surface, Mg growth at different substrate temperatures from 400 to -30°C was performed with the same magnesium flux. It is found that when the substrate temperature is above 20°C , only amorphous Mg_2Si layer forms due to the strong reactivity of Mg with Si according to the RHEED patterns and x-ray photoelectron spectra (XPS) (not shown here). The formation of disordered Mg_2Si could be completely suppressed when the substrate temperature decreases to 0°C or lower. In this case a well-defined single-crystal Mg layer forms on Si(111). Figures 1(b)–1(f) illustrate the evolution of RHEED patterns during the growth of Mg layer at -10°C . Here the (7×7) pattern is used to calibrate the Mg coverage, namely, when the (7×7) pattern disappears completely, 1 ML of Mg was supposed to deposit onto the substrate.⁹ It is obvious that the surface structure will not change before another monolayer Mg is deposited, indicating that the wetting layer growth is completed at about 2 ML. Mg starts to grow with a bulk hcp structure at 3 ML, and is fully relaxed at 4 ML according to the rod spacing of RHEED pattern, implying that a sharp interface of Mg(0001)/Si(111) forms at -10°C . When the Mg film was kept at -10°C for a couple of hours, no obvious change in the RHEED patterns was observed. It suggests that the interface is stable at LT. However, the RHEED patterns became diffused and finally halo when the temperature increased to 20°C or higher. Therefore, the Mg(0001)/Si(111) interface

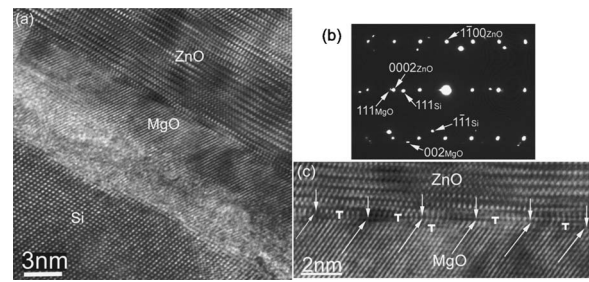


FIG. 2. Cross-sectional HRTEM micrograph along $[10\bar{1}]_{\text{Si}}$ direction near the interface region (a), corresponding SAED pattern (b), and high magnification image near the ZnO/MgO interface (c), in which a clear configuration of domain matching epitaxy of ZnO(0001) on MgO(111) is illustrated. Every 10-unit ZnO cells (marked by upper arrows) is matched with every 11-unit MgO cells (lower arrows).

structure is very sensitive to temperature and is unstable even at RT.

After the 4-nm-thick Mg(0001) film deposition at -10°C [Fig. 1(f)], oxidation of Mg film was performed at the same temperature under O^* ambient for 20 min. Figure 1(g) shows the RHEED pattern of the single-domain MgO formed. The thickness of MgO is quite limited because the oxidation is governed by diffusion.¹⁰ Therefore, the Mg layer remains below the ultrathin MgO layer and a double heterostructure of MgO(111)/Mg(0001)/Si(111) forms. With this double layer, the Si surface is free from O^* and formation of amorphous silicon oxide is prevented. In the third step, further MgO growth was performed to increase the MgO layer thickness [Fig. 1(h)] to about 6 nm, and three-dimensional islands are prevailing on the surface, which can serve as nuclei for subsequent ZnO growth. Finally, 1- μm -thick ZnO epitaxial film was grown on the MgO template. The sharp streaky lines in Figs. 1(i) and 1(j) imply that the ZnO film is single crystalline with a good quality. In the RHEED patterns, ZnO(0001), MgO(111), Mg(0001), and Si(111) are parallel with each other with an in-plane epitaxial relationship as $\langle 10\bar{1}0 \rangle_{\text{ZnO}} \parallel \langle 11\bar{2} \rangle_{\text{MgO}} \parallel \langle 10\bar{1}0 \rangle_{\text{Mg}} \parallel \langle 11\bar{2} \rangle_{\text{Si}}$ (the lattice constant for MgO versus ZnO along these directions is 5.16 versus 5.63 Å).

Figure 2 shows cross-sectional HRTEM images and corresponding selected area electron diffraction (SAED) pattern near the interface region of the ZnO sample taken along $[10\bar{1}]_{\text{Si}}$ direction. A well-defined MgO layer below ZnO and an amorphous layer above Si can be clearly seen from Fig. 2(a), suggesting that the good crystal quality of MgO is maintained during the temperature ramping and even after high-temperature growth of the ZnO epilayer, though severe degradation of the Mg(0001)/Si(111) interface occurs. The SAED pattern shown in Fig. 2(b) illustrates a rocksalt phase of MgO and a crystalline orientation relationship of $[11\bar{2}0]_{\text{ZnO}} \parallel [1\bar{1}0]_{\text{MgO}} \parallel [10\bar{1}]_{\text{Si}}$, which are consistent with the RHEED observations shown in Fig. 1. Figure 2(c) shows a sharp interface of ZnO(0001)/MgO(111). Moreover, a domain matching epitaxy (DME) of ZnO is realized on MgO(111) via matching of 10-unit ZnO cells and 11-unit MgO cells along $[1\bar{1}00]_{\text{ZnO}}$ direction resulting in only -0.8% residual strain. The DME is confirmed with the misfit dislocations in the sharp interface of MgO/ZnO, which strongly demonstrates the role of the MgO layer as a well-defined template in high crystal-quality ZnO epitaxy.

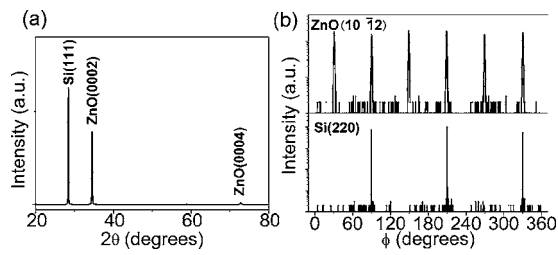


FIG. 3. XRD spectra of the ZnO film on Si(111): (a) θ - 2θ scan; (b) ϕ scans of ZnO(10 $\bar{1}2$) and Si(2 $\bar{2}0$) planes.

The crystal quality of the ZnO film is further confirmed by x-ray diffraction (XRD) measurements. Figure 3(a) shows a θ - 2θ scan of XRD, in which the sharp diffraction peaks of ZnO(0002) and ZnO(0004) indicate that the ZnO film is strictly grown along c axis without a second phase. To further study the symmetry of the ZnO film off the growth direction, Φ -scan test was performed on the ZnO(10 $\bar{1}2$) and (220) planes, respectively, by azimuthally rotating from 0° to 360° along c axis. It is obvious from Fig. 3(b) that the ZnO film has a single-domain wurtzite structure, and the surface lattices of ZnO(0002) and Si(111) are exactly overlapped without any rotation, which is consistent with the above RHEED observations.

The ZnO film is also proven to have a good optical quality by photoluminescence (PL) measurements at both 300 K [Fig. 4(a)] and 10 K [Fig. 4(b)]. No deep-level emissions are detected at 300 K. Moreover, a strong near-band-edge emission is found at 3.30 eV with a full width at half maximum (FWHM) of only 95 meV. In comparison with those of other ZnO films on Si(111) prepared by using other buffer layers, such as ZnS (>100 meV),⁶ and Si₃N₄ (110 meV),⁸ the ZnO film obtained by this LT interface technique has a superior optical quality, which is also comparable to those of ZnO bulk crystal,¹¹ and high-quality ZnO films on sapphire,¹² ScAlMgO₄,¹³ and CaF₂.¹⁴ Furthermore, at the high-energy side of the PL spectrum at 10 K [Fig. 4(b)], B free exciton (FX_B) and A free exciton (FX_A) can be distinguished clearly at 3.379 and 3.373 eV. A broad peak centered at 3.363 eV of H-donor-bound exciton emission (I_4) covers the range of 3.369–3.355 eV,¹⁵ and the free exciton emissions accompanied by single phonon (FE-1LO) and dual phonons (FE-2LO) are also observed at 3.310 and 3.238 eV with an interval of 72 meV. As the FWHM of FX_A is very sensitive to the residual strain in film,¹⁴ the narrow FWHM of 3 meV indi-

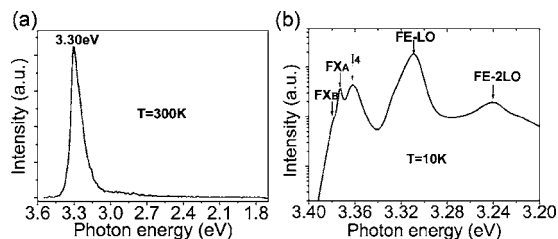


FIG. 4. PL spectra of the ZnO film on Si(111): (a) obtained at 300 K; (d) spectrum in near-band-edge region taken at 10 K.

cates that the residual strain in the ZnO film is very small.

Considering that the interface control was carried out at LT while the growth of ZnO epilayer was performed at 650°C , an important question arises: how does the MgO(111)/Mg(0001)/Si(111) structure change during the increase of temperature? Our XPS and HRTEM measurements prove that Mg₂Si layer forms due to the strong interdiffusion at 20°C or higher, resulting in a double heterostructure of MgO/Mg₂Si/Si. Surprisingly, if MgO layer is thick enough, the crystal quality of thermodynamically stable MgO layer does not degrade, which serves as a proper template for ZnO epitaxy. On the other hand, Mg₂Si will form when Mg is deposited at 20°C or higher, making the formation of high-quality MgO and ZnO difficult.

In summary, a three-step LT interface engineering method, involving LT deposition of Mg, oxidation of Mg film, and further homoepitaxy of MgO, has been developed to grow ZnO films on Si(111) by MBE. The formation of a well-defined double heterostructure of MgO(111)/Mg(0001)/Si(111) at -10°C prevents the Si surface from oxidation and serves as an excellent template for single-domain epitaxy of ZnO which shows high crystal and optical quality. This technique should also be very useful to control various reactive metal/Si interfaces to obtain high-quality oxide templates on Si substrate.

This work is financially supported by Natural Science Foundation of China, Ministry of Science and Technology of China, and Chinese Academy of Sciences.

- ¹J. H. Lim, C. K. Kang, K. K. Kim, I. K. Park, D. K. Hwang, and S. J. Park, *Adv. Mater.* (Weinheim, Ger.) **18**, 2720 (2006).
- ²Z. X. Mei, X. L. Du, Y. Wang, M. J. Ying, Z. Q. Zeng, H. Zheng, J. F. Jia, Q. K. Xue, and Z. Zhang, *Appl. Phys. Lett.* **86**, 112111 (2005).
- ³M. J. Ying, X. L. Du, Y. Z. Liu, Z. T. Zhou, Z. Q. Zeng, Z. X. Mei, J. F. Jia, H. Chen, Q. K. Xue, and Z. Zhang, *Appl. Phys. Lett.* **87**, 202107 (2005).
- ⁴K. S. An, R. J. Park, J. S. Kim, and C. Y. Park, *J. Appl. Phys.* **78**, 1151 (1995).
- ⁵M. Fujita, N. Kawamoto, M. Sasajima, and Y. Horikoshi, *J. Vac. Sci. Technol. B* **22**, 1484 (2004).
- ⁶Y. Z. Yoo, T. Sekiguchi, T. Chikyow, M. Kawasaki, T. Onuma, S. F. Chichibu, J. H. Song, and H. Koinuma, *Appl. Phys. Lett.* **84**, 502 (2004).
- ⁷J. J. Zhu, B. X. Lin, R. Yao, G. L. Zhao, and Z. X. Fu, *Chin. J. Semicond.* **25**, 1662 (2004).
- ⁸C. C. Lin, S. Y. Chen, S. Y. Cheng, and H. Y. Lee, *Appl. Phys. Lett.* **84**, 5040 (2004).
- ⁹T. Nagao, S. Ohuchi, Y. Matsuoka, and S. Hasegawa, *Surf. Sci.* **419**, 134 (1999).
- ¹⁰A. U. Goonewardene, J. Karunamuni, R. L. Kurtz, and R. L. Stockbauer, *Surf. Sci.* **501**, 102 (2002).
- ¹¹Y. Harada and S. Hashimoto, *Phys. Rev. B* **68**, 045421 (2003).
- ¹²Y. F. Chen, D. M. Bagnall, H. J. Koh, K. T. Park, K. Hiraga, Z. Zhu, and T. Yao, *J. Appl. Phys.* **84**, 3912 (1998).
- ¹³A. Tsukazaki, A. Ohtomo, T. Onuma, M. Ohtani, T. Makino, M. Sumiya, K. Ohtani, S. F. Chichibu, S. Fuke, Y. Segawa, H. Ohno, H. Koinuma, and M. Kawasaki, *Nat. Mater.* **4**, 42 (2005).
- ¹⁴H. J. Ko, Y. F. Chen, Z. Zhu, and T. Yao, *Appl. Phys. Lett.* **76**, 1905 (2000).
- ¹⁵B. K. Meyer, H. Alves, D. M. Hofmann, W. Kriegseis, D. Forster, F. Bertram, J. Christen, A. Hoffmann, M. Straßburg, M. Dworzak, and U. Haboeck, *Phys. Status Solidi B* **241**, 231 (2004).